

Effect of Atomic Layer Deposition Coatings on the Surface Structure of Anodic Aluminum Oxide Membranes

Guang Xiong,[†] Jeffrey W. Elam,[‡] Hao Feng,^{||,‡} Catherine Y. Han,[§] Hsien-Hau Wang,[§] Lennox E. Iton,[§] Larry A. Curtiss,^{*,†,§} Michael J. Pellin,[§] Mayfair Kung,^{||} Harold Kung,^{||} and Peter C. Stair^{†,||}

Chemistry Division, Argonne National Laboratory, Argonne, Illinois 60439, Energy Systems Division, Argonne National Laboratory, Argonne, Illinois 60439, Materials Science Division, Argonne National Laboratory, Argonne, Illinois 60439, Department of Chemistry and Center for Catalysis and Surface Science, Northwestern University, Evanston, Illinois 60208, and Institute for Environmental Catalysis, Northwestern University, Evanston, Illinois 60208

Received: January 19, 2005; In Final Form: March 29, 2005

Anodic aluminum oxide (AAO) membranes were characterized by UV Raman and FT-IR spectroscopies before and after coating the entire surface (including the interior pore walls) of the AAO membranes by atomic layer deposition (ALD). UV Raman reveals the presence of aluminum oxalate in bulk AAO, both before and after ALD coating with Al₂O₃, because of acid anion incorporation during the anodization process used to produce AAO membranes. The aluminum oxalate in AAO exhibits remarkable thermal stability, not totally decomposing in air until exposed to a temperature >900 °C. ALD was used to cover the surface of AAO with either Al₂O₃ or TiO₂. Uncoated AAO have FT-IR spectra with two separate types of OH stretches that can be assigned to isolated OH groups and hydrogen-bonded surface OH groups, respectively. In contrast, AAO surfaces coated by ALD with Al₂O₃ display a single, broad band of hydrogen-bonded OH groups. AAO substrates coated with TiO₂ show a more complicated behavior. UV Raman results show that very thin TiO₂ coatings (1 nm) are not stable upon annealing to 500 °C. In contrast, thicker coatings can totally cover the contaminated alumina surface and are stable at temperatures in excess of 500 °C.

1. Introduction

In recent years, there has been increasing interest in the synthesis and characterization of anodic aluminum oxidation (AAO) membranes arising from their applications as a scaffold platform for nanofabrication,¹ nanomask,² information storage,³ and catalysis.^{4,5} AAO is also used as a template structure for the fabrication of nanowires, nanotubes, nanocomposites, and so forth.^{1,6,7} The most interesting feature of AAO membranes is their highly aligned pores of uniform cylindrical shape and size. The pore size, pore density, and AAO thickness can be controlled by the anodization conditions.⁴ For example, narrow pore diameter distributions can be formed with diameters ranging from 20 to 400 nm by changing the applied potential and the electrolyte.

Potential uses of AAO membranes in separations require that there be precise control of the pore diameter. Their use in catalysis would be greatly expanded if the chemical pore wall composition could be varied arbitrarily. The compositional constraint comes because the porous oxide can be produced with only a few materials (Al, Si) and also because impurities are incorporated into the structure of AAO membranes during synthesis.^{4,8,9} The presence of the incorporated impurities could have a significant influence on the near-surface structure of the

membranes and on the catalytic and separation properties of the membranes. Therefore, it is of interest to characterize the impurities and understand their behavior under conditions to which the membrane might be exposed during use. It is also useful to either eliminate or cover the contaminated surface by annealing or by atomic layer deposition (ALD) encapsulation.

Modification of AAO membranes by ALD provides the means of controlling the pore diameter as well as the pore wall composition.^{10,11} ALD is a thin film growth technique that uses alternating, saturating reactions between gaseous precursors and a substrate to deposit films in a monolayer-by-monolayer fashion.¹² The controlled growth of thin films can be accomplished using an ABAB... binary reaction sequence. Furthermore, a wide variety of materials including oxides, nitrides, sulfides, and metals have been deposited using ALD.¹³

Recently, it has been demonstrated that ALD can uniformly coat each pore of AAO in a layer-by-layer fashion over the entire pore length.¹⁰ Nanostructured membranes, fabricated by a combination of AAO and ALD, have been used as the support for the synthesis of oxidation catalysts.¹¹ These membranes offer unique catalytic environments including (1) precisely controlled pore size, (2) tailored pore wall composition, and (3) controlled flow of reagents in and out of the catalyst.

In this paper, we report on a detailed structural study of AAO membranes before and after ALD coating using ultraviolet (UV) Raman spectroscopy and Fourier transform-infrared spectroscopy (FT-IR). The combination of these methods is used to characterize the structure of AAO membranes before and after ALD coating with both Al₂O₃ and TiO₂. ALD coating is shown

* Corresponding author.

[†] Chemistry Division, Argonne National Laboratory.

[‡] Energy Systems Division, Argonne National Laboratory.

[§] Materials Science Division, Argonne National Laboratory.

^{||} Department of Chemistry and Center for Catalysis and Surface Science, Northwestern University.

[#] Institute for Environmental Catalysis, Northwestern University.

to encapsulate incorporated anions and to produce a more uniform hydroxylated surface.

2. Experimental Section

Aluminum oxalate was purchased from Alfa Aesar and was used without further purification.

A. Synthesis of AAO. AAO membranes were synthesized by anodizing pure Al foil (0.5 mm, 99.999%, 100 × 100 mm, Sigma-Aldrich). First, the Al foils were degreased in acetone and were electrochemically polished in a polishing solution (perchloric acid:EtOH = 1:9). Next, the foil was anodically oxidized in a 0.3 M aqueous oxalic acid solution at 3 °C at a potential of 40 V. The anodization was repeated twice. The first anodization step took ~15 h. Then, the AAO film was chemically stripped by immersing the sample in a mixture of 6% phosphoric and 1.8% chromic acids. The second anodization was carried out under the same conditions as the first for an additional 24 h. This two-step anodization process greatly improves the ordering of the nanopore arrays. The remaining unreacted Al foil was etched in 0.1 M CuCl₂ 37.5% HCl solution to release the AAO membrane from the unreacted portion of the Al foil. The barrier layer, a thin oxide film that formed the interface between the Al foil and the bottoms of the nanopores, was then removed by immersing the AAO membrane in 5% H₃PO₄ at 30 °C for 70 min. This step opens the AAO membrane pores providing parallel pores open at both the top and bottom of the film. The resulting membranes are typically about 70- μ m thick.

B. Atomic Layer Deposition. The nanoporous AAO membranes were coated by Al₂O₃ and TiO₂ ALD using a viscous-flow ALD reactor operated in a quasi-static mode^{10,14} at a deposition temperature of 177 °C. The AAO substrates were placed in the reactor with the long axes of the nanopores oriented perpendicular to the carrier gas flow. Alternating exposures to trimethyl aluminum (TMA, Aldrich) and water vapor from deionized water were used for performing the Al₂O₃ ALD¹⁰ while the TiO₂ ALD utilized alternating titanium tetrachloride (TiCl₄, Aldrich) and deionized water exposures.

During each ALD cycle, the reactor was first evacuated using a mechanical pump to a pressure below 0.02 Torr. Next, the reactor was filled with the first ALD precursor to a pressure of 5 Torr for time t_1 . Following this exposure, the reactor was evacuated and then purged with ultrahigh purity nitrogen at a mass flow rate of 200 sccm and a pressure of 1 Torr for time t_2 . Next, the exposure to the second precursor was performed at 5 Torr for time t_1 , followed by evacuation and nitrogen purge for time t_2 . The exposure times and purge times were increased during the course of the coating process to account for the slower diffusion as the pores narrowed.¹⁰ The initial cycles used $t_1 = 10$ s and $t_2 = 30$ s, while the final cycles used $t_1 = 45$ s and $t_2 = 60$ s.

Al₂O₃ ALD was also used to coat a Si(111) wafer to serve as a Raman standard for amorphous alumina. This deposition was performed using the ALD reactor in a conventional flowing mode for 1000 TMA/H₂O cycles with the timing sequence 1–5–1–5 with a resulting thickness of about 130 nm.

C. Characterization of AAO membranes. *UV Raman Spectroscopy.* The UV Raman spectra were measured using a UV Raman instrument built at Northwestern University. Details of the UV Raman instrument have been provided elsewhere.^{15,16} The Raman spectra were excited at 244 nm generated by an intracavity, frequency-doubled argon ion laser (Lexel 95 SHG). The laser power at the sample is 4 mW, and a typical spectrum collection time is 20 min. The UV Raman spectra were recorded

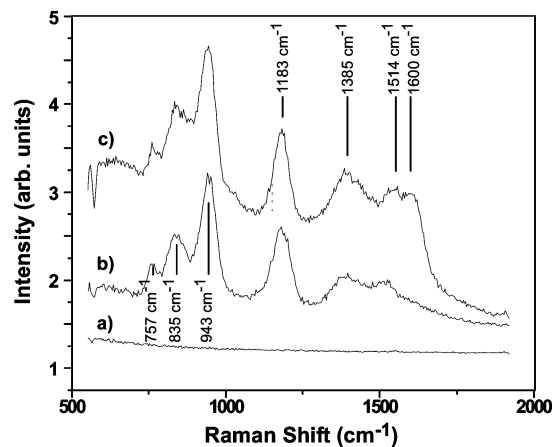


Figure 1. UV Raman spectra of (a) amorphous Al₂O₃ on Si, (b) AAO, and (c) aluminum oxalate after annealing at 550 °C in Ar.

in air. The AAO samples were 13 mm in diameter with a thickness of 70 μ m placed on top of a flat sample holder.

FT-IR. The FT-IR measurements were performed using a Nicolet 60 SX transmission FTIR spectrometer equipped with a mercury cadmium telluride (MCT) detector and a quartz cell connected to the gas manifold. The samples were calcined for 2–3 h at 450 °C in an O₂ flow and then were cooled to room temperature. All spectra were recorded in He at room temperature. Background measurement was performed using an empty cell in a He flow at room temperature. The spectra were obtained by subtracting the background from the raw data. Spectra were collected with a resolution of 4 cm⁻¹ (128 scans).

SEM. The scanning electron micrograph (SEM) images were acquired using a Hitachi S4700 SEM with a field emission gun (FEG) electron beam source.

3. Results

The UV Raman spectra of AAO, amorphous Al₂O₃, and aluminum oxalate are shown in Figure 1. Amorphous alumina Figure 1a was used as a clean reference, since AAO is also composed of amorphous alumina. The amorphous alumina was synthesized by ALD as described in the Experimental Section. The spectrum of AAO (Figure 1b) exhibits peaks at 757, 835, 943, 1183, 1385, and 1514 cm⁻¹, respectively. As shown in Figure 1a, there is no detectable signal from the amorphous Al₂O₃ sample, indicating that the peaks in the UV Raman spectrum from the AAO membrane (Figure 1b) are not from the amorphous Al₂O₃, which forms the bulk of the AAO.

It has been reported that as much as 5% of the anodized portion of the AAO membrane are acid anions incorporated into the structure of AAO membrane during anodization.^{4,8,9} These studies demonstrated that two different alumina regions are formed during the anodization process: a center framework of relatively pure alumina and a pore wall region contaminated by introduction of the acid anion. These two regions are clearly evident in SEM micrographs of uncoated AAO membranes (Figure 2a) because of their differing secondary electron yield. An example of an ALD coated AAO membrane is shown in Figure 2b. The uniformity over this region is clearly demonstrated. Cross-sectional SEM studies (not shown) demonstrate that the coating is uniform along the entire pore length.

To ascertain whether the Raman spectrum for our oxalic acid derived AAO was a result of anion incorporation, a reference compound, hydrated aluminum oxalate (Aldrich), was tested. The reference compound was dried at 550 °C in Ar and was subsequently measured using UV Raman at room temperature

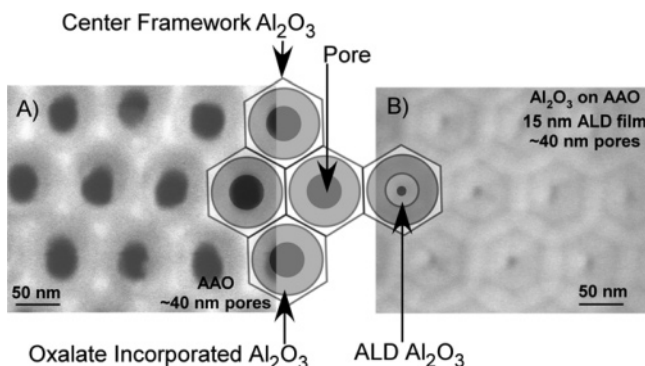


Figure 2. SEM top view micrographs of (a) an uncoated AAO and (b) a 15-nm alumina-coated (ALD) membrane showing 10-nm pores remaining. The uncoated SEM membrane shows the different secondary electron yields of the AAO membrane. The bright regions are from what is suggested to be relatively pure alumina, while the gray portion has incorporated oxalate anions. The dark portions are the pores themselves.

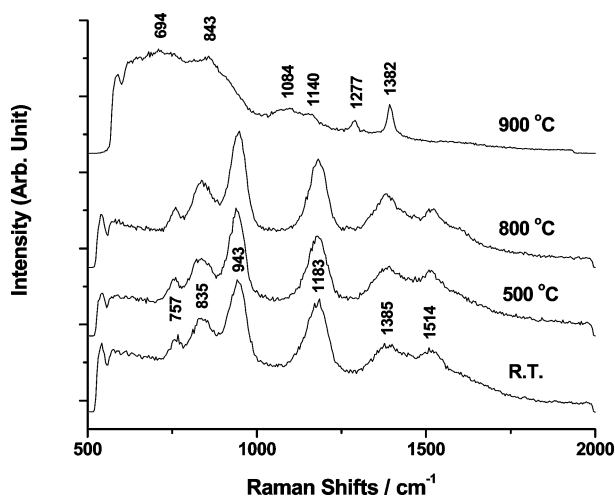


Figure 3. UV Raman spectra of an AAO membrane at room temperature after a heat treatment at room temperature (R.T.), 500 °C, 800 °C, and 900 °C in air.

under ambient conditions (Figure 1c). The Raman spectra of the dehydrated aluminum oxalate and that of AAO membrane (Figure 1b) are very similar, suggesting that the peaks from the AAO membrane can be assigned to aluminum oxalate trapped in the AAO alumina structure.

The temperature dependence of the UV Raman spectra of an AAO membrane is displayed in Figure 3. For each spectrum, the AAO membrane was calcined at the indicated temperature in flowing air for 5 h and then was cooled to room temperature before the spectrum was recorded. The spectrum of the AAO membrane remained essentially unchanged up to 800 °C and then changed significantly when annealed to 900 °C. This suggests that the trapped aluminum oxalate remained stable up to 800 °C before decomposing at 900 °C. The spectrum at 900 °C presents a broad peak ranging from 500 to 1000 cm^{-1} together with peaks at 1084, 1140, 1277, and 1382 cm^{-1} . To assign these peaks, reference spectra of α -, γ -, and δ - Al_2O_3 were acquired. In the range of 600–2000 cm^{-1} , peaks at 740 and 830 cm^{-1} were observed for δ - Al_2O_3 , and a peak at 740 cm^{-1} was found for α - Al_2O_3 . Obviously, it is difficult to confirm the presence of crystalline Al_2O_3 from the UV Raman spectra since a broad band masks every peak between 500 and 1000 cm^{-1} . However, evidence from unpublished *in situ* X-ray diffraction measurements at 900 °C establish that γ - Al_2O_3 is gradually formed.

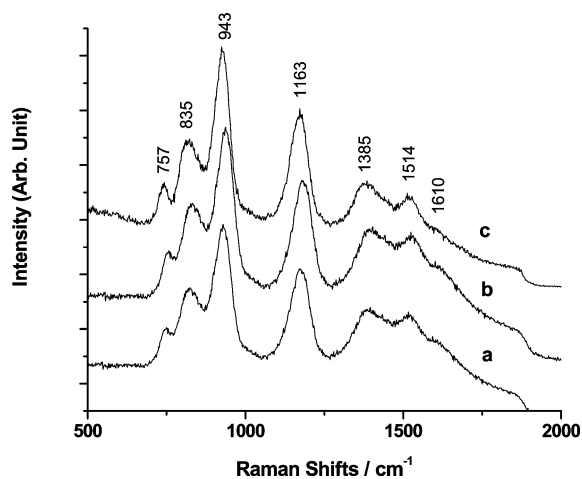


Figure 4. UV Raman spectra of (a) an AAO membrane, (b) a 15-nm ALD coating of Al_2O_3 on an AAO membrane, and (c) a 15-nm ALD coating of Al_2O_3 on an AAO membrane after annealing at 500 °C in air.

When using these membranes for catalysis, thermal decomposition of the oxalate may not be desirable for at least two reasons. First, the AAO structure may be significantly changed at the high temperatures and, second, the carbon contaminants may still be present in the AAO structure, just in a different form (possibly carbonate). Either of these scenarios could change the catalytic properties of these structures. Therefore, an alternative method that involves covering the contaminated surface using ALD was attempted. In this study, a 15-nm Al_2O_3 film was deposited on the surface of an AAO membrane. This coating reduces the pore diameter from 40 to 10 nm. Figure 4 displays the UV Raman spectra of the AAO membrane before and after the 15-nm Al_2O_3 coating. The UV Raman spectra of the coated and uncoated samples are nearly identical. This is not surprising since (1) the excitation laser and the Raman scattered signals are not absorbed by the 15-nm alumina film (alumina does not absorb UV light at 244 nm) and (2) ALD alumina coatings do not display any significant peaks (Figure 1a).

To obtain direct evidence of the ALD layer from UV Raman measurements, TiO_2 was chosen as a coating material. Because TiO_2 strongly absorbs UV light, the UV laser beam will not penetrate the TiO_2 film. Figure 5 shows the UV Raman spectra of the AAO membrane coated by a 1-nm TiO_2 film. The intensities of aluminum oxalate UV Raman peaks are greatly reduced. (Figure 5b) This indicates that the UV Raman spectrum samples only the near surface region of the TiO_2 coated sample. After annealing at 500 °C, the peaks of aluminum oxalate return. This result suggests that TiO_2 dissolves into the bulk of the alumina or forms clusters on the surface during annealing, exposing the underlying aluminum oxalate.

Figure 6 exhibits the UV Raman spectra of an AAO membrane coated with a two-layer ALD film comprised of a 1-nm Al_2O_3 film and a 14-nm TiO_2 film. The 1-nm Al_2O_3 film allows coating of the TiO_2 film on a compositionally uniform Al_2O_3 film. The sharp peak at 1550 cm^{-1} is from O_2 in the air. No peak associated with aluminum oxalate is detectable at either room temperature (R.T.) or 500 °C. This result indicates that the thicker coating can totally cover the contaminated alumina surface. Furthermore, the outer surface of the composite membrane remains intact as a complete layer of TiO_2 after annealing to 500 °C. This does not preclude the possibility of some subsurface interfacial mixing of the TiO_2 and Al_2O_3 having occurred.

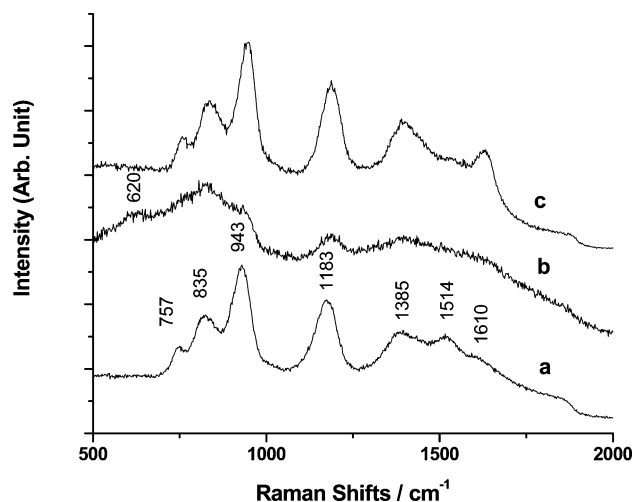


Figure 5. UV Raman spectra of (a) an AAO membrane, (b) a 1-nm ALD coating of TiO₂ on an AAO membrane, and (c) a 1-nm ALD coating of TiO₂ on an AAO membrane after annealing at 500 °C.

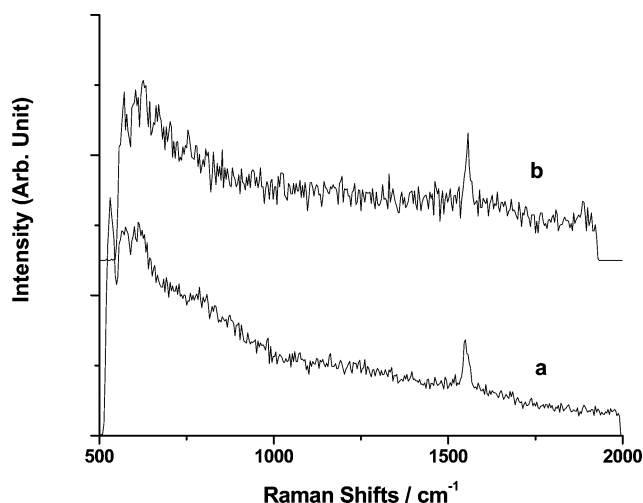


Figure 6. UV Raman spectra of (a) a 14-nm ALD coating of TiO₂ on a 1-nm ALD coating of Al₂O₃ on an AAO membrane (b) sample in (a) after annealing at 500 °C in air.

The FT-IR spectra of AAO membranes dehydrated at 450 °C for 2 h in O₂ followed by cooling to R.T. are shown in Figure 7. A commercial AAO membrane (Whatman) was measured under the same conditions (Figure 7c). The spectra of our AAO membranes and the commercial (Whatman) membranes exhibit FT-IR bands at 3556, 3677, 3746, and 3793 cm⁻¹. Following the literature assignments,^{17–19} the peaks at 3677, 3746, and 3793 cm⁻¹ are assigned to three types of isolated hydroxyl groups, which are bound to three, two, and one aluminum atoms, respectively. The broad band at 3556 cm⁻¹ is associated with hydrogen-bonded hydroxyl groups. Generally, the hydroxyl group peaks are broad, but the bands assigned to isolated hydroxyl groups in Figure 7b and c are relatively sharp, indicating that the AAO surface is very uniform. After coating by ALD, all peaks of the isolated OH groups disappear and only that of the hydrogen-bonded OH group was observed. This suggests that all hydroxyl groups are in environments where the hydroxyl density is high enough for hydrogen bonding and that the number of more isolated hydroxyl group sites has substantially decreased. The lack of isolated hydroxyl group sites indicates that the ALD alumina coatings are free of defects which lead to missing hydroxyls.

The temperature dependence of the UV Raman spectra of aluminum oxalate powder is shown in Figure 8. The hydrated

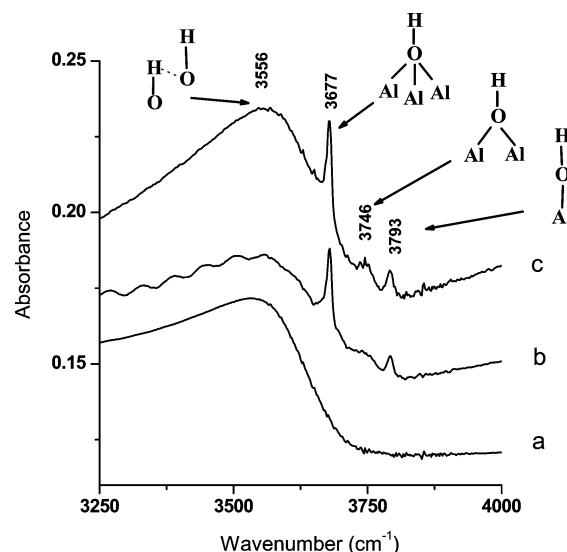


Figure 7. FT-IR spectra of (a) a 15-nm ALD coating of Al₂O₃ on an AAO membrane, (b) an uncoated AAO membrane, and (c) an Anopore porous membrane (Whatman). All spectra are taken after annealing at 450 °C in O₂.

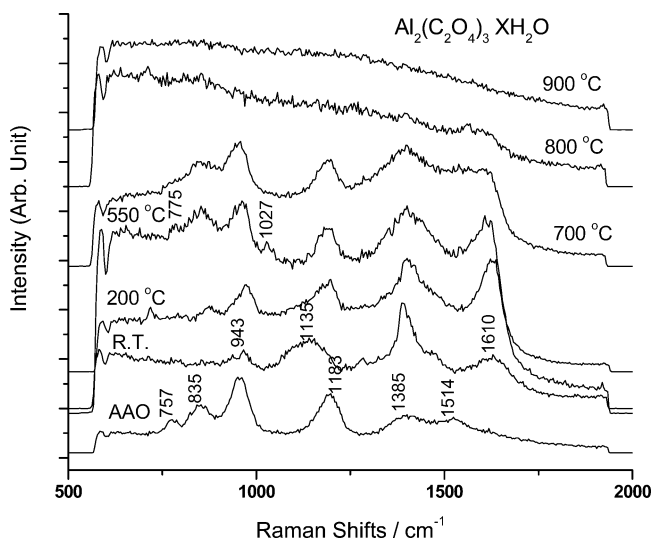


Figure 8. UV Raman spectra of aluminum oxalate powder after annealing in dry air at different temperatures. The bottom spectrum is of an AAO membrane calcined to 550 °C shown for comparison.

aluminum oxalate at room temperature exhibits peaks at 950, 1135, 1375, and 1610 cm⁻¹. After calcining to 200 °C, a new peak at 860 cm⁻¹ appears, the peak at 950 cm⁻¹ intensifies, and the peak at 1135 cm⁻¹ shifts to 1181 cm⁻¹. After annealing at 550 °C, peaks at 775 and 1027 cm⁻¹ appear. The spectrum at 550 °C is similar to that of the AAO membrane. After annealing at 800 and 900 °C, all the sharp peaks disappear indicating decomposition of the oxalate.

4. Discussion

The UV Raman results confirm that acid anions are incorporated into the structure of AAO membranes. The spectrum of the trapped anions in AAO is very similar to that of aluminum oxalate after annealing at 550 °C. The decomposition temperature of the aluminum oxalate in AAO is 900 °C (see Figure 3). Xu et al.⁹ demonstrated by thermogravimetric analysis that a weight loss in AAO membranes (produced in oxalic acid) takes place at 890–930 °C, which is the same as the decomposition temperature observed in this study. From the compari-

son between Figure 3 and Figure 8, it is clearly seen that the decomposition temperature of aluminum oxalate in AAO is higher than that of aluminum oxalate powder, indicating that the aluminum oxalate in AAO is somewhat more stable. This is probably because most of the aluminum oxalate in the bulk of AAO cannot directly contact O₂ in air.

Since annealing does not decompose contaminate anions until high temperature, ALD is an alternative method to obtain a compositionally uniform pore wall surface. The UV Raman results show that a 1-nm TiO₂ layer can cover the contaminated surface but that this film is not stable upon annealing to 500 °C. Ti atoms may dissolve into bulk alumina or aggregate to form TiO₂ nanoparticles on the surface. In contrast, a 15-nm titania layer is quite stable even upon calcination to 500 °C continuing to cover the pore walls.

ALD coating of AAO membranes not only forms a compositionally uniform surface but also modifies the types of hydroxyl groups present on the surface. Hydroxyl groups play an important role in surface chemistry and catalysis. For example, hydroxyl groups can be acidic or basic, which is reflected in their vibrational frequencies, and can be the active sites in catalytic reactions. Moreover, the preparation of catalysts using impregnation or grafting methods²⁰ is carried out through the interaction of precursor chemicals with hydroxyl groups. Following Al₂O₃ coating of AAO by ALD, the isolated hydroxyl groups disappear and only hydrogen-bonded hydroxyl groups are observed. This suggests that ALD coating of AAO by Al₂O₃ produces a more uniform surface layer.

5. Conclusions

Anodic aluminum oxide (AAO) membranes were characterized by UV Raman and FT-IR spectroscopies before and after coating the entire surface (including the interior pore walls) of the AAO membranes by atomic layer deposition (ALD). The UV Raman spectrum of AAO membrane gives direct evidence that dehydrated aluminum oxalate is incorporated into the structure of AAO because of acid anion incorporation during the anodization process. The elimination of the contaminant anions can be accomplished only by annealing to high temperature. The decomposition of the trapped aluminum oxalate starts at 550 °C but is not completed until 900 °C. Since annealing does not remove contaminate anions until high temperature,

ALD is an alternative method to obtain a compositionally uniform pore wall surface. A 15-nm titania layer was found to totally cover the contaminated alumina surface. Coating of AAO membranes by ALD not only forms a compositionally uniform surface but also modifies the types of hydroxyl groups present on the surface.

Acknowledgment. This work was supported by the U.S. Department of Energy Basic Energy Sciences under Contract No. W-31-109-ENG-38. The SEM analysis was performed in the Electron Microscopy Center, Materials Science Division, Argonne National Laboratory, Argonne, IL.

References and Notes

- (1) Chen, R.; Xu, D.; Guo, G.; Gui, L. *J. Mater. Chem.* **2002**, *12*, 2435.
- (2) Masuda, H.; Watanabe, M.; Yasui, K.; Tryk, D.; Rao, T.; Fujishima, A. *Adv. Mater. (Weinheim, Germany)* **2000**, *12*, 444.
- (3) AlMawlawi, D.; Coombs, N.; Moskovits, M. *J. Appl. Phys.* **1991**, *70*, 4421.
- (4) O'Sullivan, J. P.; Wood, G. C. *Proc. R. Soc. London, Ser. A* **1970**, *317*, 511.
- (5) Patermarakis, G.; Pavlidou, C. *J. Catal.* **1994**, *147*, 140.
- (6) Yin, A. J.; Li, J.; Jian, W.; Bennett, A. J.; Xu, J. M. *Appl. Phys. Lett.* **2001**, *79*, 1039.
- (7) Steinhart, M.; Wendorff, J. H.; Greiner, A.; Wehrspohn, R. B.; Nielsch, K.; Schilling, J.; Choi, J.; Goesele, U. *Science* **2002**, *296*, 1997.
- (8) Thompson, G. E.; Wood, G. C. *Nature* **1981**, *290*, 230.
- (9) Xu, T.; Zhao, J. Z.; Cheng J. M.; Dang, H. X. *J. Trace Microprobe Tech.* **1997**, *15*, 521.
- (10) Elam, J. W.; Routkevitch, D.; P. P. Mardilovich; George, S. M. *Chem. Mater.* **2003**, *15*, 3507.
- (11) Pellin, M. J.; Stair, P. C.; Xiong, G.; Elam, J. W.; Birrell, J.; Curtiss, L.; George, S. F.; Hahn, C. T.; Iton, L.; Kung, L.; Kung, H.; Wang, H. *Catal. Lett.*, in press.
- (12) George, S. M.; Ott, A. W.; Klaus, J. W. *J. Phys. Chem.* **1996**, *100*, 13121.
- (13) Ritala, M.; Leskela, M. Atomic Layer Deposition. In *Handbook of Thin Film Materials*; Nalwa, H. S., Ed.; Academic Press: San Diego, CA, 2001; Vol. 1.
- (14) Elam, J. W.; Groner, M. D.; George, S. M. *Rev. Sci. Instrum.* **2002**, *73*, 2981.
- (15) Chua, Y. T.; Stair, P. C. *J. Catal.* **2000**, *196*, 66.
- (16) Chua, Y. T.; Stair, P. C.; Wachs, I. E. *J. Phys. Chem. B* **2001**, *105*, 8600.
- (17) Knoezinger, H.; Ratnasamy, P. *Catal. Rev.—Sci. Eng.* **1978**, *17*, 31.
- (18) Tsyganenko, A. A.; Mardilovich, P. P. *J. Chem. Soc., Faraday Trans.* **1996**, *92*, 4843.
- (19) Liu, X.; Truitt, R. E. *J. Am. Chem. Soc.* **1997**, *119*, 9856.
- (20) Weckhuysen, B. M.; Keller, D. E. *Catal. Today* **2003**, *78*, 25.